Investigation of the thermal cycling durability of cobonded piezoelectric sensors for the shm of reusable launch vehicles

Loïc Mastromatteo, Ludovic Gaverina, Florian Lavelle, Jean-Michel Roche, François-Xavier Irisarri

INVESTIGATION OF THE THERMAL CYCLING DURABILITY OF COBONDED PIEZOELECTRIC SENSORS FOR THE SHM OF REUSABLE LAUNCH VEHICLES

Loïc MASTROMATTEO [(1)], Ludovic GAVERINA [(1)], Florian LAVELLE [(2)], Jean-Michel ROCHE [(1)], François-Xavier IRISARRI [(1)]

[(1)] DMAS, ONERA, Paris-Saclay University, 29 Av. de la Division Leclerc, F-92322 Châtillon, FRANCE,
Email: loic.mastromatteo@onera.fr
[(2)] CNES, 52 Rue Jacques Hillairet,75012 Paris, FRANCE,
Email: florian.lavelle@cnes.fr

KEYWORDS

Cobonded sensors, Electro-Mechanical Impedance (EMI), Guided Waves (GW), Laser Doppler Vibrometry (LDV), Reusable Launch Vehicle (RLV), Carbon Fiber Reinforce Polymer (CFRP)

ABSTRACT

This paper addresses the durability of cobonded PZT transducers for Guided Waves Structural Health Monitoring under thermal cycles partially representative of an RLV use case. The evolution of the transducers' response is characterized using three different approaches. First, Laser Doppler Vibrometry imaging and electromechanical impedance spectrum monitoring are used to diagnose and identify potential bonding defects of the transducers, as these are one of the main durability issues for the SHM sensors. Then the effects on transducer performance are investigated by measuring guided wave pitch-catch signals in a composite plate. The results are compared with previous works using secondary bonded PZT, since secondary bonding is the classic method for surface mounted transducers. The advantages of the cobonding process are discussed in comparison to classic secondary bonding in the optics of RLV applications.

1. INTRODUCTION

Over the past decade, the development of reusable launch vehicles (RLVs) to reduce the cost of access to orbit has become a strategic concern for the space industry. However, to achieve this goal, the additional cost of reusability (recuperation and revalidation of stages between launches) must be as low as possible. In this context, Structural Health Monitoring (SHM) systems could help to optimize inspection and maintenance operations on structures. One of the techniques commonly used in SHM is based on the propagation of guided waves (GW) in structures [1]. Sensor networks (such as networks of piezoelectric PZT patches) can detect the interaction of GW with structural defects (cracks, delamination in composites, etc.), allowing their localization.

One of the main challenges for these systems is the durability of the sensors under environmental and operational conditions [2]. SHM systems are often based on a comparison with a reference state of the structure (ideally without defects). Therefore, it is important that the output of the sensors does not change significantly during the life cycle of the structure to reduce the risk of false detection due to a degraded sensor condition. One of the critical issues for GW sensors is the mechanical coupling between the sensors themselves and the host structure in which GW will propagate. PZT transducers are often coupled to the host structure by a secondary bonding process with an additional adhesive layer. However, the degradation of this adhesive layer can significantly affect the performance of SHM systems, and bonding defects are one of the main durability issues for the sensors in the literature. Specifically for composite structures, an alternative to the secondary bonding process is the cobonding process, in which the sensor is applied directly to the uncured composite. The sensor and host structure are then cured together, with the sensor being bonded by the matrix of the composite material. This process, which avoids the use of an additional adhesive layer, could help increase the durability and reliability of the bond between the sensor and structure. To the best of our knowledge, few papers have investigated the durability of cobonded PZT transducers and discussed their interest, let alone for RLV applications. Therefore, this work focuses on testing a cobonding process for PZT transducers and investigating their durability under thermal cycling. The temperature cycles are chosen to be representative of the thermal stresses that some areas of an actual RLV composite structure under the thermal protection might be subjected to: limited number of cycles (about 10) of short duration (5 minutes) and high temperatures (150°C). This work follows a previous study on the durability of secondary bonded PZT transducers under the same conditions [3] and is based on the same experimental methodology to allow a proper comparison between both bonding methods. The approach followed in this work consists in applying laser heating cycles to PZT transducers cobonded to a CFRP plate to monitor the evolution of their responses, using different techniques: local vibration laser Doppler vibrometry (LDV) imaging,

electromechanical impedance (EMI) [4] and GW pitch catch measurements. The first two techniques are used to detect and identify degradations of the PZT bonding condition [5], [6]; the monitoring of GW amplitudes in emission and reception enables to evaluate the performance of the PZT during thermal cycling.

The present paper is organized as follows. Section 2 discusses the interest of the cobonding process for RLV applications in relation to the literature, Section 3 presents the experimental methodology and describes the three different characterization methods. The results for cobonded sensors are presented in Section 4 and compared to the results previously observed for secondary bonded sensors. Finally, conclusions and future works are discussed in Section 5.

2. SENSORS COBONDING PROCESS

When monitoring a system with a sensor, it is critical for the sensor to be properly coupled to the physical phenomenon it is designed to measure. In the case of vibration-based SHM, the mechanical coupling between the sensors and the structure is the key parameter. In SHM, the sensors are usually coupled with the structure through a secondary bonding process that requires an additional adhesive layer between the sensor and the structure. The design, control, and validation of the bonding process is a real concern for the reliability and durability of SHM systems, and rightly so, bonding failures are one of the most critical sensor failures cited and studied in the literature. For metallic structures, the secondary bonding process is mandatory, but for organic matrix composite structures, there are other alternatives, such as a full embedding inside the composite material or an intermediate solution, the co-bonding process.

In [7], the opportunities offered by the cobonding process were analysed and discussed from an industrialization perspective. In addition to the higher automation possibilities (compared to secondary bonding), a reduction of manual labour and infrastructure due to a lower number of manufacturing steps was mentioned, as the cobonding process largely coincides with the curing process of the host structure. In terms of durability and reliability, this reduced process complexity and manual labour could likely lead to a more controlled and reproducible process. Especially because most of the bonding process is merged with the host structure curing process, which is very well known and controlled. In addition, the cobonding process eliminates the secondary adhesive layer, reducing to one the number of interfaces that could potentially fail during the life of the system. Lastly,for cobonded PZT, if the sensor diagnostic reveals a change of the mechanical properties of the “adhesive layer”, this would directly mean that the mechanical properties of the composite matrix are affected and confusion with a degradation of the secondary adhesive layer is eliminated.
According to [8] in which cobonded PZT transducers were tested under mechanical fatigue loading, no bonding degradation was observed and sensor failures occurred due to cracks in the brittle PZT ceramic after high number of fatigue cycles. However, in RLV applications, the structures and the sensors will complete only a few dozen launches, so that fatigue is not as relevant as for aircraft applications associated with several thousands of flight hours. This shorter life cycle could also help reduce the need to replace the sensors, which is beneficial since repairability is one of the challenges of the cobonding process.

Another challenge of the cobonding process is the effect that it might have on the mechanical properties of the host structure due to possible fiber misalignment under the PZT as it can be seen in Figure 1 [7].

Figure 1: Fiber misalignment under a cobonded sensor [7]

Finally, a specificity of the cobonding process is that it must be planned before the structure is produced, so it cannot be applied to existing structures and requires rethinking the already existing manufacturing chain, as discussed in [7] for the aircraft industry. However, there are few existing structures or established manufacturing chains for RLV applications, especially for the use of composite materials. Therefore, future developments of composite structures for RLV applications offer interesting opportunities to include SHM systems from the start and produce smart structures easier to inspect and revalidate.

It is important to note that although this work focuses on the durability of cobonded transducers for GW SHM, the cobonding process can also be used for other types of sensors and SHM systems such as optical fibre sensors for temperature or strain monitoring.

3. METHODOLOGY

Apart from the bonding process, the experimental methodology is the same as in the work presented in [3] to allow comparison of results.

3.1. Materials and PZT layout

The sensors used in this study are C-6 PZT discs from FUJI -Ceramics (diameter of 20 mm and 200

µm thick). Five of these sensors are cobonded on a 350 mm x 400 mm layered T700/M21GC CFRP composite plate (see Figure 2). The quasi-isotropic layout is $[0,-45,90,45]_s$ with a total thickness of 2 mm. The sensors are arranged in a 30° tilted square to reduce direct wave reflections, and PZT#1 in the centre is used as a reference PZT to transmit and receive guided waves. The other PZT discs are coated with black paint to control surface emissivity during thermal cycling.

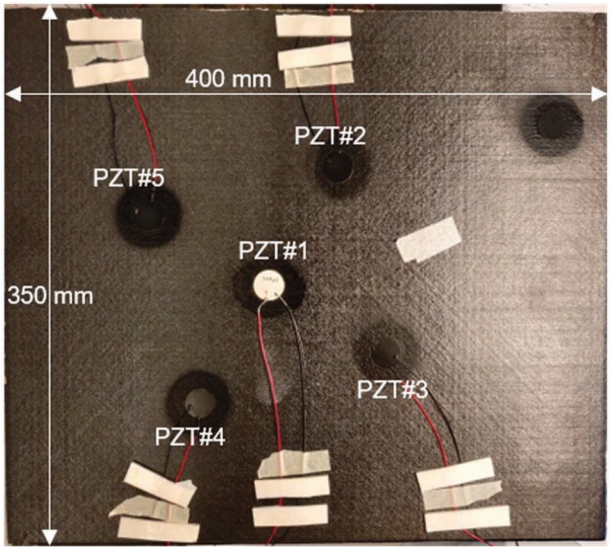

Figure 2: PZT layout on the composite plate

3.2. Cobonding process

The cobonding process starts with the cleaning of the PZT discs with a solvent. They are then dried to ensure that no impurities are present and placed directly on the uncured layered material. The top side of the sensors is covered with a Kapton tape to protect the contact points from possible resin leakage during the curing process. The remaining part of the bonding process lies in the manufacturing of the host composite structure. The last key-point is to ensure that the positions of the sensors are not modified during the preparation for the autoclaving process.

After the curing process, the Kapton tape can be removed and the electrical connection to the electrodes of the PZTs can be soldered.

As mentioned earlier, the risk of fibre displacement under the cobonded sensors, that might happen if the PZT discs are pressed too deeply into the composite material during the autoclaving process, needs to be checked. To that extent, the thickness of the plate with the cobonded sensors is measured with a double-sided profilometer (see Figure 3). Since the thickness of the PZT discs is known ($200\ \mu m$), it is possible to determine how far the PZTs have sunk into the composite plate by comparing the average thickness of the PZT area for each PZT (red circles on the image) with the average thickness of the plate around the PZT (square areas around the PZT). The penetration depths of each PZT are listed in Tableau 1.

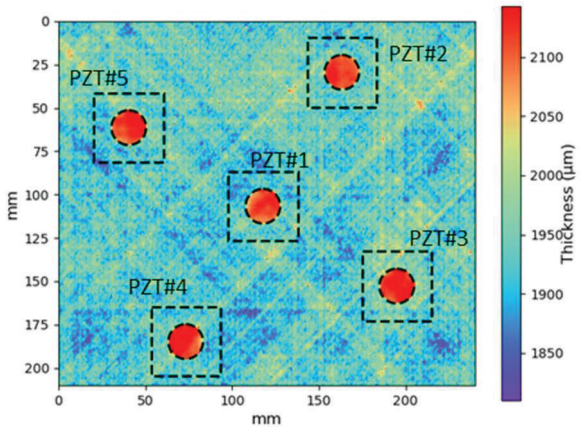

Figure 3: Thickness map of the composite plate with cobonded PZT

Tableau 1: Depth of penetration into the plate for each PZT

PZT#1	-26.3 µm
PZT#2	-13.7 µm
PZT#3	-2.6 µm
PZT#4	-2.7 µm
PZT#5	-12.1 µm

We can see that no PZT penetrated more than 26 µm into the plate, which is about one tenth of a ply thickness (250 µm) therefore the potential fiber misalignment appears negligeable. This could be due to the fact that the PZTs used for this work are quite thin and have a comparatively high surface area, so that the pressure is better distributed over the composite material, resulting in a penetration more limited than in the example shown in Figure 1.

3.3. Thermal cycling setup

The thermal cycle was chosen to be as representative as possible of a thermal environment that RLV composite components might be exposed to during their life cycle of around ten flights of a few minutes each. In contrast to this short exposure time, the thermal loads are intense (high maximum temperatures and steep thermal ramps, as seen in Figure 4) compared to other studies in the literature [9], [10], which often focus on aircraft applications and have much longer and smoother thermal cycles.

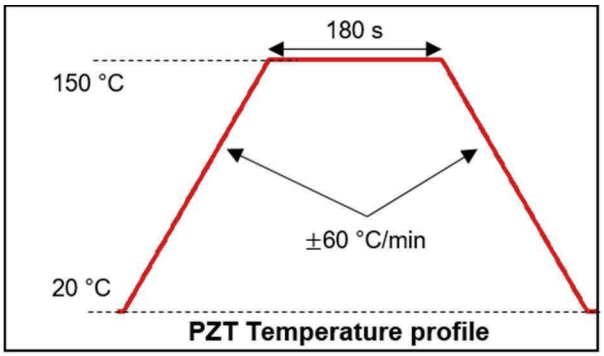

Figure 4: Targeted thermal profile at the composite surface [3]

Ten cycles are applied to PZT #2 to #5, generated using a CO_2 laser while the backside of the plate is cooled with compressed air in order to reach thermal equilibrium and have stable backside surface temperature during the cycles. Laser heating has several advantages in our case. First, it allows much steeper thermal ramps than a furnace; second, the generated heating is non-uniform, presenting a thermal gradient between the hot side (where the transducers are located) and the cold side of the coupon. This is typical of the thermal profiles RLV structures are exposed to, as the heat comes from the outside due to the backfiring of the engines while the inside is generally much cooler due to the cryogenic ergols. Finally, the Laser heating makes it possible to apply cycles to one transducer at a time without affecting the others, so the reference transducer remains undamaged. Each of the tested PZT is characterized with LDV and GW measurements in their initial state and after 5 and 10 cycles while the EMI spectrum is continuously monitored throughout the thermal cycling as presented Figure 5.

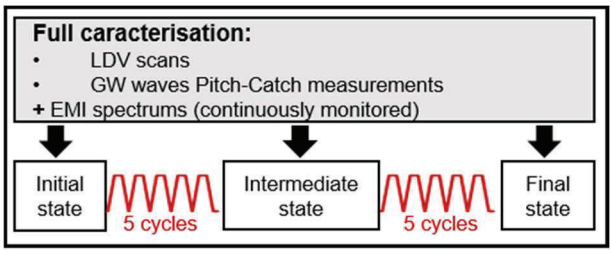

Figure 5: Thermal cycling workflow

Methods and measurements used to characterize the sensors are detailed in the following section.

3.4. Sensor characterization

3.4.1. Sensor diagnosis

Two methods are used to diagnose the health and bonding conditions of the sensors: LDV and EMI.

LDV is a non-destructive test method for measuring the normal velocity of a surface. The velocity is derived from the Doppler frequency shift of the laser beam scattered from the surface. In this work, LDV is used to detect possible bond defects caused by the initial bonding process or by thermal cycling. The detached parts of the PZT discs are expected to have a higher amplitude of local vibrations since the adhesive does not restrain them. These higher amplitude zones can be easily identified on the root mean square velocity images, as shown in [11], [3]. Thus, LDV measurements allow the identification of small bonding defects in surface-mounted PZT sensors. Although this technique is not applicable in operational conditions because the sensors are likely to be covered by a protective thermal barrier, it is useful to understand the sensor debonding phenomena and to validate the second diagnosis technique, the EMI method.

This EMI method is based on the fact that when a PZT is coupled with a host structure, its electrical impedance is related to the mechanical impedance of the structure through the piezoelectric effect that generates a coupling between the mechanical and electrical variables. In the SHM field, the EMI method is often used for damage detection [12] but can also be used for the transducers assembly self-diagnosis by identifying the signatures of possible sensor debondings or degradations in the impedance or admittance spectra [5], [6]. In this study, the electrical admittance spectra are measured in the [80 - 440] kHz range, using an HP 4194A Impedance Analyzer. This frequency range is chosen to include the main resonance of the PZT transducers and the signature of potential debonding. As the PZT and the host structure form a coupled system, this frequency range of interest will strongly depend on the sensors (geometry, piezoelectric properties…) and the mechanical properties of the host structure.

3.4.2. Sensor performance evaluation

The targeted application for that kind of PZT transducers are guided waves based SHM systems. Thus, it is interesting to look at their capabilities to emit and receive guided waves into the host structure. Due to the presence of a reference, undamaged PZT, it is possible to test the PZT discs both in reception and in emission as presented Figure 6. The output signals are normalized with the input maximum amplitudes and the relative amplitudes (V_{in}/V_{out}) are measured in the initial state and after 5 and 10 thermal cycles.

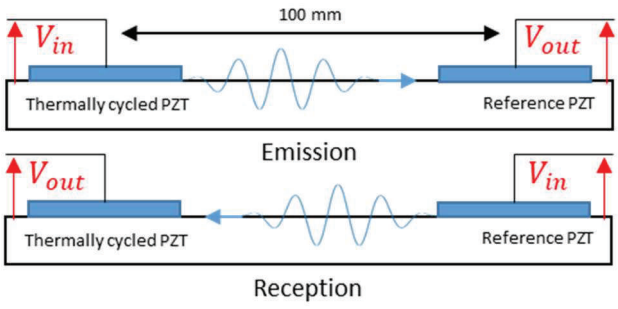

Figure 6: Emission and reception configurations

PZT input voltage is a 5-cycle Hanning windowed sinusoidal toneburst at 10 V peak-to-peak. In GW SHM, in order to avoid complex mode superposition, the frequency range is often limited to have only the two fundamental Lamb wave modes, namely the first antisymmetric (A0) and symmetric (S0) modes. For our composite plate, this limits the frequency at around 350 kHz. Therefore, three measurements are done in the [15-25] kHz range (maximum A0 amplitudes) and three in the [150-250] kHz range (maximum S0 amplitudes).

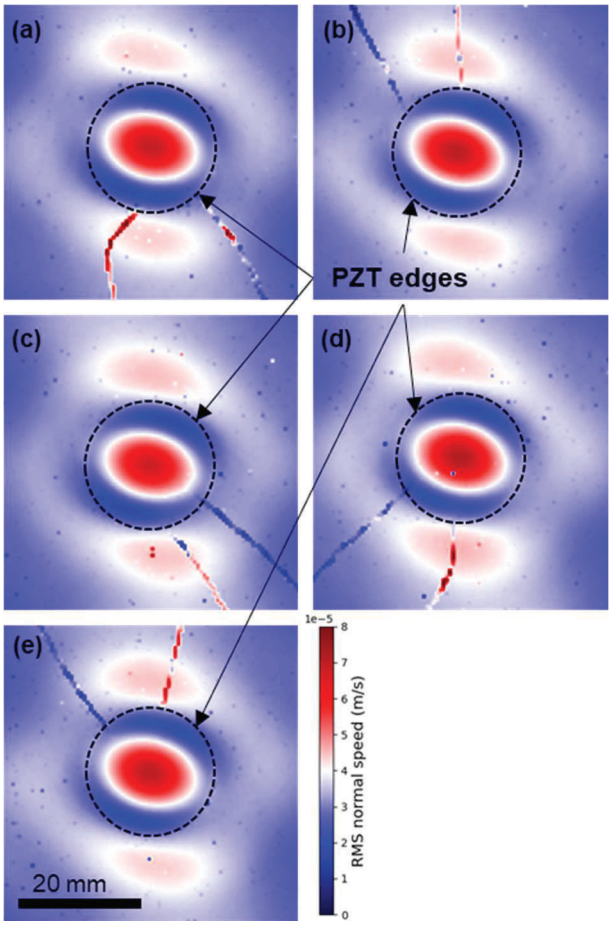

Figure 7: LDV scans in, PZT#1 to #5 areas - respectively (a) to (e) - before thermal cycling

4. RESULTS & DISCUSSIONS

The results for the cobonded PZT will be compared with the result for secondary bonded PZT from a previous work [3]. In this previous work, the transducers were bonded using a consumer grade cyanoacrylate adhesive (Loctite 495) which was quite sensible to the thermal cycling. Obviously, it would be possible to optimize the adhesive choice and improve the secondary bonding protocol to increase the reproducibility and the stability under the thermal loads. Nevertheless, this would require additional design and manufacturing work while the cobonding process is already mutualized with the structural design (material choice) and manufacturing (curing of the host structure).

4.1. Initial state diagnosis

Before any thermal cycling, initial measurements are carried out to characterize the reference state of the PZT transducers after the cobonding process. The LDV scans for the five PZT discs in their initial state are shown Figure 7.

The first thing that can be noticed is that the amplitude and spatial distribution of the out-of-plane vibrations are very similar for all the PZT discs. In addition, there are no higher amplitude zones with discontinuities that would indicate some debonding of the sensors. In comparison, Figure 8 shows the same type of scans for secondary bonded PZT from previous work [3] in which half of the sensors were showing some small debondings. The higher amplitude zones that indicates the presence of debondings (circled in yellow) can be clearly identified and the impact on the spatial distribution of the out-of-plane vibrations is seen. However, for the PZT discs without debondings, the amplitude and spatial distribution of the plate vibrations is very similar to the cobonded PZT discs.

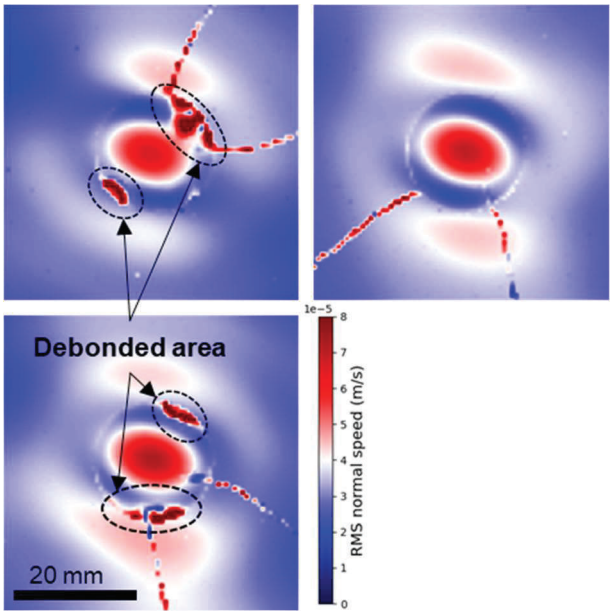

Figure 8: LDV scans for secondary bonded PZT with and without debondings [3]

The conductance spectra shown in Figure 9 are another way to evaluate the state of the sensors and their coupling with the structure after the bonding process.

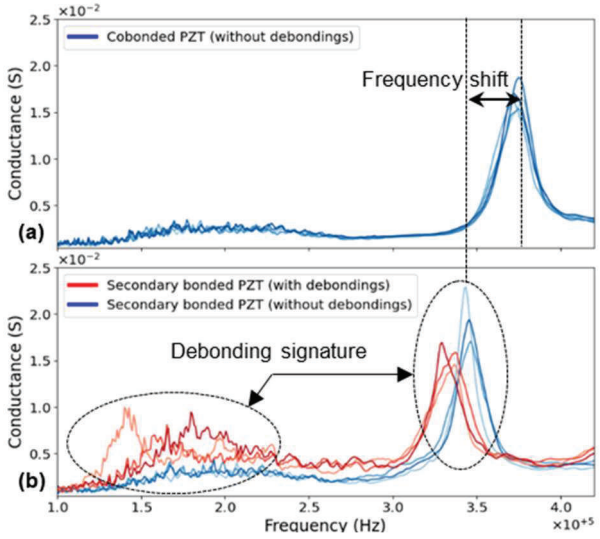

Figure 9: Conductance spectrum for cobonded PZT (a) and secondary bonded PZT (b)

For the cobonded PZT discs, the measurements are once again very similar to each other with only some slight amplitude differences located around the resonance frequency. The comparison between the cobonded and secondary bonded PZT spectra highlights a shift of the resonance frequency likely due to a higher shear stiffness between the sensor and the structure for the cobonded process. It can also be seen for the secondary bonded PZT discs, that the conductance spectra significantly change depending on the presence or absence of local debondings. Those debondings cause a reduction of amplitude and frequency of the main resonance, and also lead to the appearance of another smaller resonance at lower frequencies between 100 kHz and 250 kHz. Thus, monitoring those features can help identifying initial debonding caused by the manufacturing or detect the debonding of a sensor during the lifetime of the SHM system.

To summarize this initial diagnosis step, the cobonding method seems to help with the reproducibility of the bonding with no debonding spotted on the initial LDV scans and very similar admittance spectra for the 5 cobonded PZT. In contrast, with the secondary bonded PZT showing some initial debondings and more variability in the admittance spectra.

4.2. Evolution with thermal cycling

The LDV scans of the 4 cobonded PZT discs after 5 and 10 thermal cycles show no evolution neither in amplitude nor in the spatial distribution in the plate. This is illustrated in Figure 10 for PZT#4.

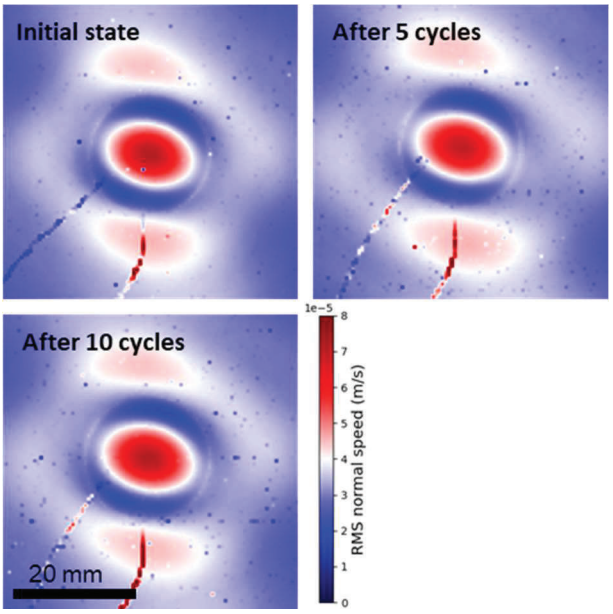

Figure 10: LDV scans for PZT#4 after 0, 5 and 10 thermal cycles

These LDV scans show no evidence of debonding during the thermal cycling for cobonded sensors. This is in contrast with the secondary bonded sensors for which additional debonding due to thermal cycling was spotted [3].
LDV measurements are relevant to locate debondings but cannot detect other changes that could affect the PZT performance, such as the evolution of the mechanical properties of the bonding layer. The admittance spectra, on the contrary, are expected to be sensitive to the evolution of the bonding layer properties. Figure 11 shows a comparison of those spectra for a secondary bonded PZT (without debonding) and cobonded PZT#4 (again, all four cobonded PZT discs show similar behaviours).

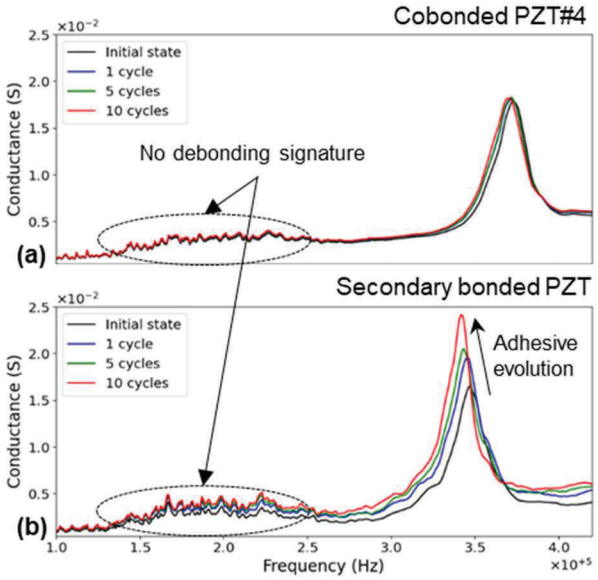

Figure 11: Conductance spectra at different thermal cycling stages for a cobonded PZT (a) and a secondary bonded PZT (b)

As expected given the LDV scans, it can be noticed that none of the PZT discs presented in Figure 11 show debonding signatures in the [100-250] kHz range. However, the evolutions around the main resonance frequency are quite different: for the cobonded PZT disc, the entire spectrum is stable throughout the thermal cycling while for the bonded one, a significant evolution of the resonant peak can be seen with an increased amplitude and a frequency downshift. This evolution is likely due to the impact of the thermal cycling on the adhesive layer's mechanical properties. The cyanoacrylate adhesive used in this previous work polymerises at ambient temperature and is likely less stable at high temperature than the epoxy matrix that is cured at 180°C during the autoclave process.

Although a difference can be identified on the admittance spectra, the most important criterion from a SHM standpoint is whether this difference impacts the guided waves performances of the sensors or not. Figure 12 shows the amplitude variation (compared to the initial state) of the guided waves emitted and received after 5 and 10 thermal cycles for the same PZT discs than in Figure 11.

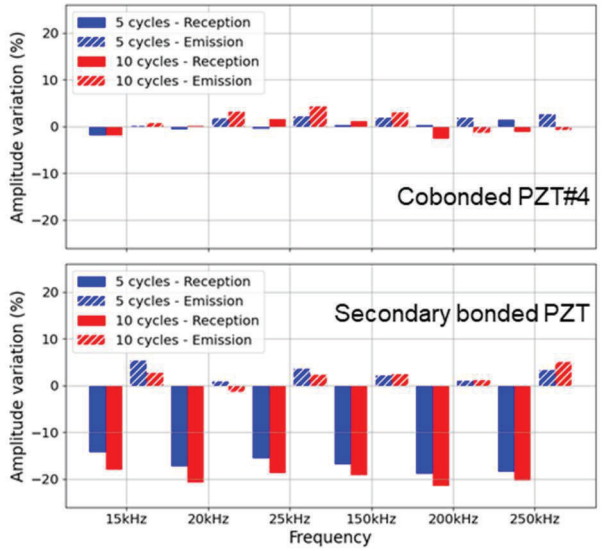

Figure 12: Impact of thermal cycling on GW emission and reception for a cobonded PZT and a secondary bonded PZT

Major differences are spotted regarding the guided waves performances. On the one hand, cobonded PZT discs present only a few percent variation of amplitude between the initial state and after 10 thermal cycles, without a clear visible tendency. On the other hand, the secondary bonded PZT discs are strongly impacted by the thermal cycles, with a 15 % to 20 % drop of amplitude for the reception capabilities. Thus, it seems that the evolution visible in the conductance spectra correlates with the evolution of the performances of the transducers regarding GW reception. The link between those measurements is essential in order to be able to use the EMI spectra for the diagnosis of GW PZT transducers.

As for the amplitude of emitted GW, no significant evolution with the thermal cycling is detected. This is quite interesting from a SHM standpoint because although the secondary bonded PZT discs are less performant in GW reception their emission performances remain unaffected. Thus, it means that when using the PZT as a source of GW, the energy sent into the host structure will not be impacted and thus the GW interactions with the structure and potential flaws will stay identical. This would be especially important when there are some non-linear interactions between the GW and the defect (e.g. crack, delamination…). However, if the PZT discs are intended to be used as passive acoustic monitoring system, the cobonding process should be preferred since it would offer better stability and reliability than the secondary bonding process.

Lastly, it is important to note that in this work we are only looking at the maximum amplitude of the guided wave signals. However, depending on how the data will be processed by a given SHM system to detect or localize a defect, other metrics or features of the GW signals could be relevant such as the waves time of flight, phase and so on. Any feature that can be affected at the same time by the degradation of the sensor and the presence of a defect is important because the risk of mix-up between a degraded sensor and a presence of damage in the host structure must absolutely be avoided.

5. CONCLUSIONS AND PERSPECTIVES

In this paper, the potential of the cobonding process to attach SHM PZT sensors to RLV composite structures was discussed in comparison with the classic secondary bonding process. The durability under thermal cycling of cobonded sensors was tested and compared to previous works carried out on secondary bonded PZT discs.

First, from a manufacturing standpoint, the cobonding process was proven faster and produced a more reproducible bonding than the secondary bonding process thanks to less manufacturing steps and a better control over the curing process as it is paired with the curing process of the host structure.

Second, regarding the durability stake, the cobonded PZT sensors submitted to thermal cycling did not show any significant evolution neither on their performances to emit and receive guided waves in the host structure, nor on the LDV and EMI measurements used to diagnose the state of the sensors. This is in stark contrast with the results obtained for secondary bonded PZT in a previous work [3] in which significant impacts were visible due to debondings and to an evolution of the adhesive layer properties. Although work could be

done to optimize the secondary bonding process for a specific use case (more suitable adhesive or surface preparation for example), the cobonding process showed a better durability and reproducibility of the bonding with a simpler and easily implemented process as most of the work is already done for the manufacturing of the host structure.

In this study, only thermal stresses were considered, but under operating conditions, transducers will also be subjected to vibration or mechanical stresses that could affect the durability of the sensors coupling with the host structure. Thus, further work is needed to confirm the potential of the cobonding process under such environment.

6. REFERENCES

[1] M. Mitra and S. Gopalakrishnan, 'Guided wave based structural health monitoring: A review', *Smart Mater. Struct.*, vol. 25, no. 5, p. 053001, May 2016, doi: 10.1088/0964-1726/25/5/053001.

[2] R. Gorgin, Y. Luo, and Z. Wu, 'Environmental and operational conditions effects on Lamb wave based structural health monitoring systems: A review', *Ultrasonics*, vol. 105, p. 106114, Jul. 2020, doi: 10.1016/j.ultras.2020.106114.

[3] L. Mastromatteo, L. Gaverina, F. Lavelle, J.-M. Roche, and F.-X. Irisarri, 'Thermal Cycling Durability of Bonded PZT Transducers Used for the SHM of Reusable Launch Vehicles', in *European Workshop on Structural Health Monitoring*, vol. 254, P. Rizzo and A. Milazzo, Eds. Cham: Springer International Publishing, 2023, pp. 727–736. doi: 10.1007/978-3-031-07258-1_73.

[4] S. Bhalla and C. K. Soh, 'Electromechanical Impedance Modeling for Adhesively Bonded Piezo-Transducers', *Journal of Intelligent Material Systems and Structures*, vol. 15, no. 12, pp. 955–972, Dec. 2004, doi: 10.1177/1045389X04046309.

[5] S. Park, G. Park, C.-B. Yun, and C. R. Farrar, 'Sensor Self-diagnosis Using a Modified Impedance Model for Active Sensing-based Structural Health Monitoring', *Structural Health Monitoring*, vol. 8, no. 1, pp. 71–82, Jan. 2009, doi: 10.1177/1475921708094792.

[6] X. Jiang, X. Zhang, T. Tang, and Y. Zhang, 'Electromechanical impedance based self-diagnosis of piezoelectric smart structure using principal component analysis and LibSVM', *Sci Rep*, vol. 11, no. 1, p. 11345, Dec. 2021, doi: 10.1038/s41598-021-90567-y.

[7] N. Dobmann, M. Bach, and B. Ekcstein, 'Challenges of an Industrialized Acousto-Ultrasonic Sensor System Installation on Primary Aircraft Structure', presented at the EWSHM 2014, Nantes, 2014.

[8] M. Moix-Bonet, I. Buethe, M. Bach, C.-P. Fritzen, and P. Wierach, 'Durability of Co-bonded Piezoelectric Transducers', *Procedia Technology*, vol. 15, pp. 638–647, 2014, doi: 10.1016/j.protcy.2014.09.025.

[9] M. Salmanpour, Z. Sharif Khodaei, and M. Aliabadi, 'Airborne Transducer Integrity under Operational Environment for Structural Health Monitoring', *Sensors*, vol. 16, no. 12, p. 2110, Dec. 2016, doi: 10.3390/s16122110.

[10] X. Liu, Y. Xu, X. Wang, Y. Ran, and W. Zhang, 'Effect of Adhesive and Its Aging on the Performance of Piezoelectric Sensors in Structural Health Monitoring Systems', *Metals*, vol. 10, no. 10, p. 1342, Oct. 2020, doi: 10.3390/met10101342.

[11] I. Mueller and C.-P. Fritzen, 'Inspection of Piezoceramic Transducers Used for Structural Health Monitoring', *Materials*, vol. 10, no. 1, p. 71, Jan. 2017, doi: 10.3390/ma10010071.

[12] W. Na and J. Baek, 'A Review of the Piezoelectric Electromechanical Impedance Based Structural Health Monitoring Technique for Engineering Structures', *Sensors*, vol. 18, no. 5, p. 1307, Apr. 2018, doi: 10.3390/s18051307.